Shear Instabilities in the Atmosphere in the Presence of a Jump in the Brunt-Väisälä Frequency

C. PELLACANI, C. TEBALDI AND E. TOSI

Istituto di Fisica A. Righi, Università di Bologna, 40126 Bologna, Italy

(Manuscript received 20 June 1977, in final form 9 May 1978)

ABSTRACT

The stability properties of a Helmholtz velocity profile in a stratified, Boussinesq fluid are investigated in the presence of a jump in the Brunt-Väisälä (BV) frequency at a level different from the one where the vortex sheet is located. New unstable modes in the range of low horizontal wavenumbers are found with respect to the case where no BV frequency jump exists. The structure of the associated unstable disturbances is similar to that of neutrally propagating gravity waves. The associated growth rates are rather small but significant because they appear in a range of horizontal wavenumbers which are otherwise stable.

A comparison with the results obtained by Lindzen and Rosenthal and by Lalas *et al.* shows a strict analogy with the study of the stability properties of a Helmholtz velocity profile in the presence of a lower rigid boundary. The generation of such instabilities is interpreted in terms of multiple overreflexions at the shear interface due to the presence of the reflecting BV frequency jump for neutral propagating waves. Applications for values of the relevant parameters suitable to actual atmospheric cases are discussed.

1. Introduction

Kelvin–Helmholtz (KH) instabilities are responsible for many detected phenomena in the free atmosphere such as billow clouds, clear-air turbulence and gravity wave radiation (Ludlam, 1967; Sekioka, 1970; Lindzen, 1974). The basic mechanism of generation of such instabilities was discovered by Helmholtz (1868) and his theory has since been extended by others. A complete review of the subject has been presented by Drazin and Howard (1966). Many improvements of the theory were induced to take into account observational data obtained in the atmosphere by new experimental remote sensing apparatus (lidar, acoustic radar, FM–CW radar).

Recently, to explain the characteristics of internal waves observed in unstable atmospheric shear zones, Lindzen (1974) investigated the stability properties of a Helmholtz velocity profile in an infinite Boussinesq fluid with constant Brunt–Väisälä (BV) frequency. In the case considered by Lindzen, instability can be predicted for perturbations with zero horizontal phase speed and horizontal wavenumbers greater than a critical value k_c given by

$$k_c^2 = N^2/2U^2, \tag{1}$$

where $2U$ is the jump in mean horizontal velocity and N the BV frequency of the fluid. Also, making use of a two-layer model, Einaudi and Lalas (1974) investigated the effect of condensation on the properties of KH instabilities of a Helmholtz profile in an infinite fluid. A net effect of the condensation was the change of the effective BV frequency in one of the two semi-infinite layers. In this way jumps in both the BV frequency and mean horizontal velocity were present at the same interface. Remarkable departures from Lindzen's results were observed by Einaudi and Lalas in the characteristics of the instability, the most interesting feature being the presence of new unstable modes due to the jump in the BV frequency.

The results obtained by Lindzen and by Einaudi and Lalas can be applied to a wide class of observed physical situations. At the same time, the importance of the role played by gravity waves in influencing mesoscale weather systems has been recently confirmed in investigations by many authors (Uccellini, 1973; Bosart and Cussen, 1973; Keliher, 1975), particularly in the range of long horizontal wavelengths (1–100 km). Stability analysis of common atmospheric situations against gravity-type disturbances is then important to give a plausible physical explanation of the mechanism of generation of detected gravity waves. The extension of the theory proposed in this paper is to consider the effect on the stability of a BV jump at a height different from the one where a localized shear zone is located. This case also resembles many physical situations observed in the atmosphere.

0022-4928/78/1633-1643$05.50

Results of recent studies on the instability induced by the presence of a rigid lower boundary on a Helmholtz velocity profile in a semi-infinite fluid with constant BV frequency have shown that the presence of such a rigid bottom significantly affects the stability of the whole system (Lindzen and Rosenthal, 1976; Lalas *et al.*, 1976; Davis and Peltier, 1976). Thus the various authors have shown that the value of unstable horizontal wavenumbers (as well as their associated growth rates) at a localized shear layer in the atmosphere are affected by the presence of the ground. The effect of the ground is mathematically taken into account by the introduction of proper boundary conditions at the ground level. In almost the same way, the existence of a BV frequency jump at a height different from that where a shear layer exists introduces (in a layered model) new matching conditions for the solutions, while boundary conditions at infinity are not affected.

In the next sections it will be shown that this BV frequency jump effect has to be taken into account to interpret observational data in the atmosphere. It is finally suggested that tropopause folding, usually associated with cyclogenesis, would cause a net destabilization of preexisting tropospheric shear layers in the range of low horizontal wavenumbers.

2. The model and the governing equations

We make use of a two-dimensional, three-layer model represented in Fig. 1. The lower semi-infinite layer A is characterized by a constant value of the BV frequency $N_A=N_1$ and a constant mean horizontal velocity $U_{0A}=-U$. The value of the BV frequency in the intermediate layer B is again constant ($N_B=N_1$) while the mean horizontal velocity is $U_{0B}=U$. The upper semi-infinite layer C is characterized by a BV frequency $N_C=N_2\neq N_1$ and a mean horizontal velocity $U_{0C}=U$. The shear zone is then represented by the interface between layers A and B, while the BV frequency jump is represented by the interface between layers B and C.

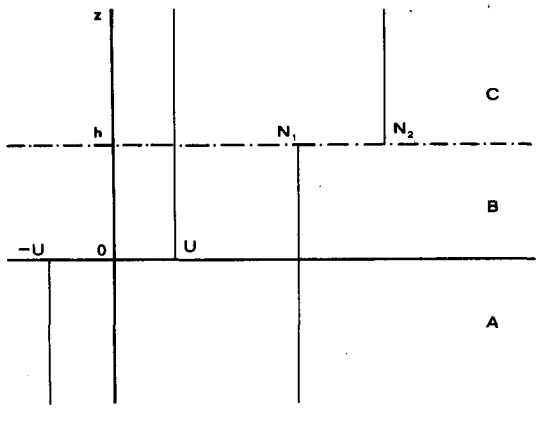

FIG. 1. The two-dimensional, three-layer model.

Since the perturbations of interest have horizontal wavelengths >10 m and associated velocities of the order of 1 m s^{-1}, we can reasonably make use of the Boussinesq approximation. From the basic equations, so simplified, one obtains (Lindzen, 1974) the differential equation

$$\left[\left(\frac{D}{Dt}\right)^2\left(\frac{\partial^2}{\partial x^2}+\frac{\partial^2}{\partial z^2}\right)+N^2\frac{\partial^2}{\partial x^2}\right]w=0, \tag{2}$$

where D/Dt represents the usual Stokes operator

$$\frac{D}{Dt}=\frac{\partial}{\partial t}+U_0\frac{\partial}{\partial x},$$

U_0 is the mean horizontal velocity, N the BV frequency

$$N=\left(-\frac{g}{\rho_0}\frac{d\rho_0}{dz}\right)^{\frac{1}{2}},$$

ρ_0 the mean density, g the acceleration of gravity, and w the vertical component of the perturbations velocity. In deriving (2) it has also been assumed that $d^2U_0/dz^2=0$ everywhere.

We look for two-dimensional plane wave solutions of (2) of the form

$$(u,w,\rho,p)=(\hat{u},\hat{w},\hat{\rho},\hat{p})\exp[i(kx-\omega t)], \tag{3}$$

where u, w, ρ and p are the perturbations in horizontal velocity, vertical velocity, density and pressure, respectively; $\hat{u}$, $\hat{w}$, $\hat{\rho}$ and $\hat{p}$ are functions of the vertical coordinate only; and k and ω are the horizontal wavenumber and the frequency of oscillation, respectively. Using (3), Eq. (2) is reduced to a second-order ordinary differential equation

$$\left[\frac{d}{dz^2}+k^2\left(\frac{N^2}{\Omega^2}-1\right)\right]\hat{w}=0, \tag{4}$$

where $\Omega=\omega-kU_0$.

Eq. (4) holds in each of the three layers of our model. Since two interfaces exist, matching conditions must be introduced; specifically, the vertical displacement and the total pressure must be continuous at each interface. Such conditions are as follows (Chandrasekhar, 1961):

Kinetic condition

$$\delta_f\left(\frac{\hat{w}}{\Omega}\right)=0 \tag{5}$$

Dynamic condition

$$\delta_f\left(\rho_0\Omega\frac{d\hat{w}}{dz}+\rho_0 k\hat{w}\frac{dU_0}{dz}\right)=gk^2\delta_f(\rho_0)\left(\frac{\hat{w}}{\Omega}\right)_f. \tag{6}$$

Here $\delta_f(f)$ is the jump a quantity experiences at the interface and $(f)_f$ is the value at the interface of a quantity which is known to be continuous there.

Solutions of (4) have to be found in each of the layers of our model and conditions (5) and (6) must be applied at both the interfaces. Solutions of (4) in each layer have the form

$$\hat{w}_I(z)=A_1^I\exp(i\gamma_I z)+A_2^I\exp(-i\gamma_I z), \tag{7}$$

where I=A, B, C and A_1^I and A_2^I are arbitrary constants. The vertical wavenumber γ_I, for the Ith layer is given by

$$\gamma_I=\pm k\left(\frac{N_I^2}{\Omega_I^2}-1\right)^{\frac{1}{2}}, \tag{7a}$$

where N_I and Ω_I are, respectively, the values of the BV frequency and of the Doppler frequency in the same layer.

It can be seen that one of the terms of (7) must vanish in each of the layers A and C because of the boundary conditions (see below) and that, if matching conditions are applied to the solutions, the following dispersion relation is obtained:

$$\begin{aligned}\Omega_-^2\gamma_B\gamma_C r-\Omega_+^2\gamma_A\gamma_B+igk^2(r-1)\gamma_B\\ +[-\Omega_-^2\gamma_B^2+\Omega_+^2\gamma_A\gamma_C r\\ +i(\Omega_+/\Omega_-)^2\gamma_A gk^2(r-1)]i\tan\gamma_B h=0,\end{aligned} \tag{8}$$

where $\Omega_+=\omega+kU$, $\Omega_-=\omega-kU$, and r is the ratio between the average values of the density above and below the BV frequency jump. The same expression (8) of the dispersion relation holds (apart from obvious exchanges of indexes) in the case where

$$N'_A=N_2,\quad U'=U,$$
$$N'_B=N_1,\quad r'=\rho_{0A}/\rho_{0B}=1/r,$$
$$N'_C=N_1,\quad h'=h.$$

The results presented in the next paragraphs are then valid for this last case as well.

The dispersion relation (8) has to be analyzed numerically to identify unstable horizontal wavenumbers and to evaluate the corresponding growth rates. To select those solutions of (8) with a valid physical meaning, radiation conditions are to be introduced together with the conditions of finiteness of solutions at infinity. For complex values of γ_A and γ_C we will then take into account solutions vanishing at $-\infty$ and $+\infty$, respectively. This implies that only one term on the right-hand side of (7) has to be retained in layers A and C; choosing the term with the positive exponential in both layers, appropriate solutions will be those satisfying the conditions

$$\mathrm{Im}(\gamma_A)<0,\quad \mathrm{Im}(\gamma_C)>0. \tag{9}$$

For real γ_A and γ_C and $\mathrm{Im}(\omega)=0$, radiation conditions are to be applied; group velocity of the solutions must, in fact, be directed upward in the upper layer C and downward in the lower layer A.

The dispersion relation in each of the two layers is given by

$$(\omega-kU_0)^2=\frac{N^2k^2}{k^2+\gamma^2}$$

so that the vertical component of the group velocity is given by

$$w_g=\frac{\partial\omega}{\partial\gamma}=-\frac{N^2k^2}{\left(\frac{\omega}{k}-U_0\right)(k^2+\gamma^2)^2}\gamma$$

and it is easily seen that the radiation conditions are

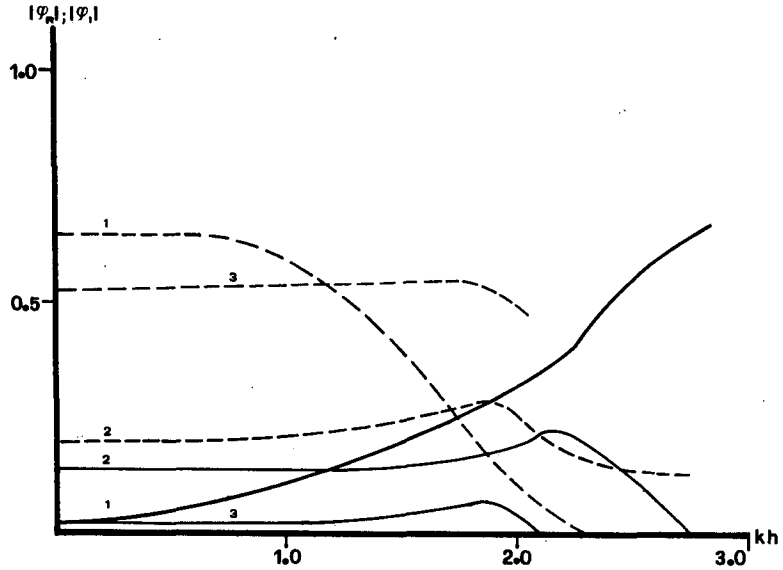

FIG. 2. Properties of unstable waves for $\alpha=0.5$ and $\beta=3$. Absolute values of $\varphi_i=\mathrm{Im}(\omega)/kU$ (solid lines) and $\varphi_r=\mathrm{Re}(\omega)/kU$ (dashed lines) are shown for different unstable modes as functions of the normalized horizontal wavenumber kh.

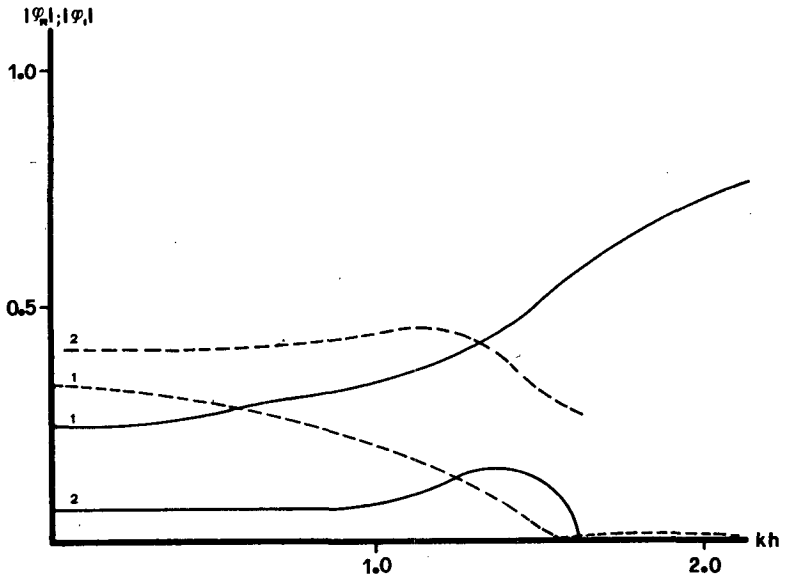

FIG. 3. As in Fig. 2 except for $\alpha=0.5$ and $\beta=2$.

satisfied for

$$\gamma_A>0, \quad \gamma_C>0. \tag{10}$$

3. Results

To investigate the possible existence of unstable modes, numerical calculations were carried out making use of the false position method (see the Appendix). Solutions were worked out for different values of the relevant physical parameters N_1, N_2, U, h and r.

The normalized imaginary part of the frequency of oscillation $\varphi_i=\mathrm{Im}(\omega)/kU$ and the normalized horizontal phase speed of numerically evaluated solutions are shown in Figs. 2–8 as functions of the nondimensional wavenumber kh for different values of the relevant nondimensional parameters α, β and r, where

$$\alpha=\frac{N_1}{N_2}, \quad \beta=\frac{N_1 h}{U}.$$

In Fig. 2 φ_i and φ_r are plotted for different modes for $\alpha=0.5$ and $\beta=3$ as functions of the nondimensional horizontal wavenumbers kh. Fig. 3 shows the behavior of the same quantities for $\alpha=0.5$ and $\beta=2$. Figs. 4 and 5 represent results obtained, respectively, for $\alpha=0.25$, $\beta=3$, $\alpha=4$ and $\beta=8$. Most of the unstable modes obtained are shown in all of the figures while, in some of the figures, all of the modes numerically worked out are represented to show the typical modal structure

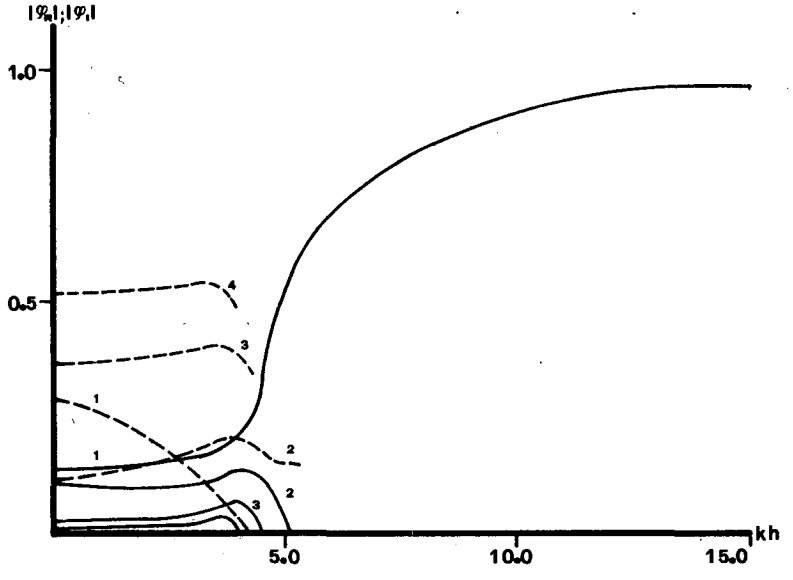

FIG. 4. As in Fig. 2 except for $\alpha=0.2$ and $\beta=6$.

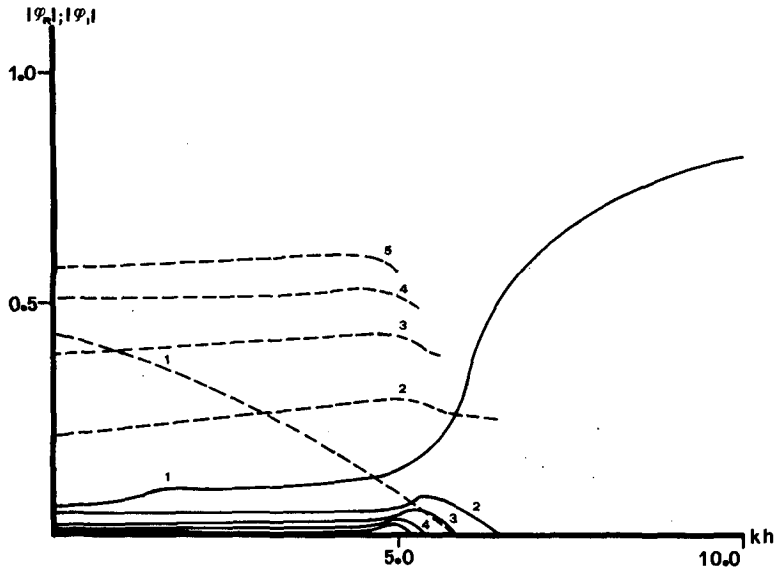

FIG. 5. As in Fig. 2 except for $\alpha=0.4$ and $\beta=8$.

of instability. Figs. 6 and 7 refer to the cases $\alpha=0.5$ and $\beta=10$ and 15, respectively, while in Fig. 8 φ_i and φ_r of solutions are plotted for $\alpha=0.25$ and $\beta=0$.

Results plotted in Fig. 9 have been obtained for a case previously investigated by Lindzen (1974). There is complete agreement between our results and those given by Lindzen. In particular, it is easily seen in Fig. 9 that instability for perturbations with zero horizontal phase speed is predicted for disturbances with horizontal wavenumbers greater than a critical value k_c given by (1). This seems to be a good test of the validity of the program for numerical solution of (8).

Figs. 10–12 show the real and imaginary parts of vertical wavenumbers of the solutions in the different layers of our model corresponding to the different modes plotted in Fig. 2. All the results described above have been worked out for $r=0.98$; other numerical experiments, not presented here, have shown that relatively large changes in r do not significantly affect the results as long as $h\neq 0$.

It must also be noted that all of the unstable modes obtained numerically satisfy the semicircle theorem (Howard, 1961). One of the most interesting features of our results is the existence of different unstable modes in the range of low horizontal wavenumbers in cases represented in most of the figures. Such modes do not appear in the case represented in Fig. 9 where

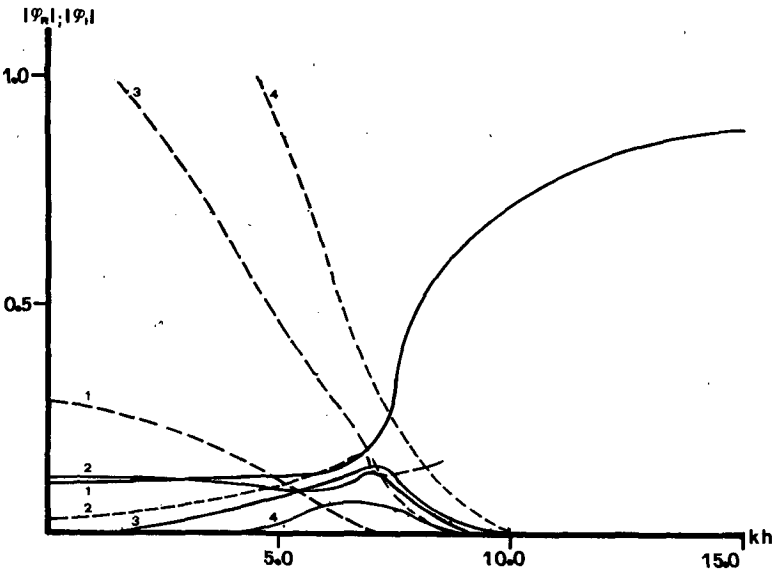

FIG. 6. As in Fig. 2 except for $\alpha=0.5$ and $\beta=10$.

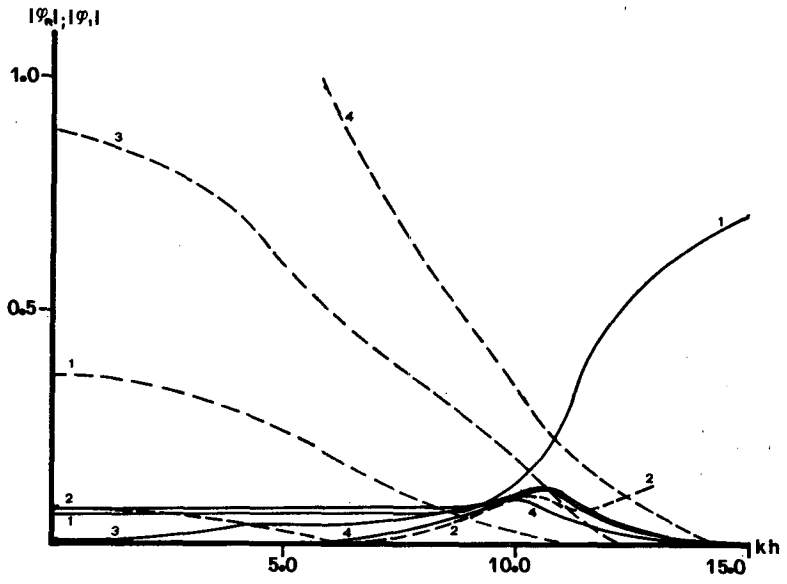

FIG. 7. As in Fig. 2 except for $\alpha=0.5$ and $\beta=15$.

no BV frequency jump exists. Growth rates $Uk\varphi_i$ associated with such new modes are rather small (usually $\varphi_i<0.2$) but significant, especially because they appear in the range of k which is otherwise stable.

Let us consider first the mode, always present, similar to the single unstable mode obtained with no BV frequency jump (see Fig. 9). The ratio between the real and the imaginary parts of the vertical wavenumbers of the unstable solutions exhibits, both above and below the shear zone, values smaller than unity for a wide range of horizontal wavenumbers; in this range disturbances are then strongly damped along the vertical direction on a length scale smaller than that of the oscillation. For low values of k, the same quantity is larger than unity; the disturbances are then damped, along the vertical direction, on a length scale greater than that of oscillation (see Figs. 10–12). Hereafter these modes will be called KH modes and the part characterized by values of $\mathrm{Re}(\gamma)/\mathrm{Im}(\gamma)$ larger than unity will be called gravity-like extensions of the KH modes. For modes other than KH modes it is seen that the ratios between the real and imaginary parts of the vertical wavenumbers above and below the shear layer always exhibit values greater than unity. The features just described suggest that disturbance associated with these new modes (as well as those associated to the gravity-like extensions of the KH modes) show a structure similar to that of vertically propagating

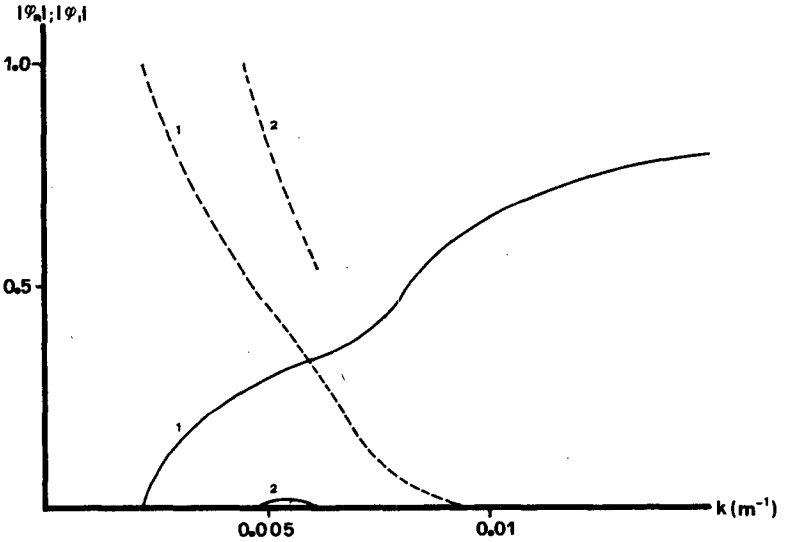

FIG. 8. As in Fig. 2 except for $\alpha=0.2$ and $\beta=0$. The results are plotted as a function of the dimensional horizontal wavenumber k.

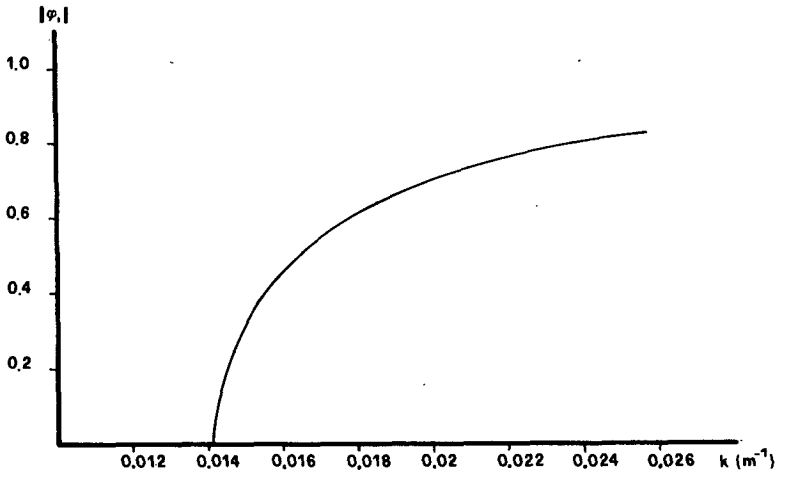

FIG. 9. Stability curve. The absolute value of $\varphi_i = \mathrm{Im}(\omega)/kU$ is plotted as a function of the wavenumber k for $N_1 = 0.02$ and $U = 1$.

gravity waves and hereafter we will call them gravity instabilities.

By inspection of Figs. 2–6 one can also notice that the normalized growth rates associated with each unstable gravity mode always exhibit a maximum which lies below the value of φ_i associated with the KH mode for the same k. It should finally be pointed out that we have modeled a localized shear zone in the atmosphere by a jump in mean horizontal velocity. This kind of model is valid only when the shear is concentrated over a height smaller than the vertical wavelengths of the disturbances of interest. As a consequence, it turns out that those ranges of unstable modes with associated small vertical wavenumbers are poorly represented by our model. An analogous effect is associated with the presence of a BV frequency jump.

4. Discussion

The physical interpretation of our results can be attempted by taking into account the following basic features:

1) The gravity-like extensions of the KH modes and the new unstable model are effects of the presence of the BV frequency jump at $z = h$.

2) The structure of such unstable disturbances is similar to that of vertically propagating waves.

3) Such unstable modes disappear for $h = 0$; in this

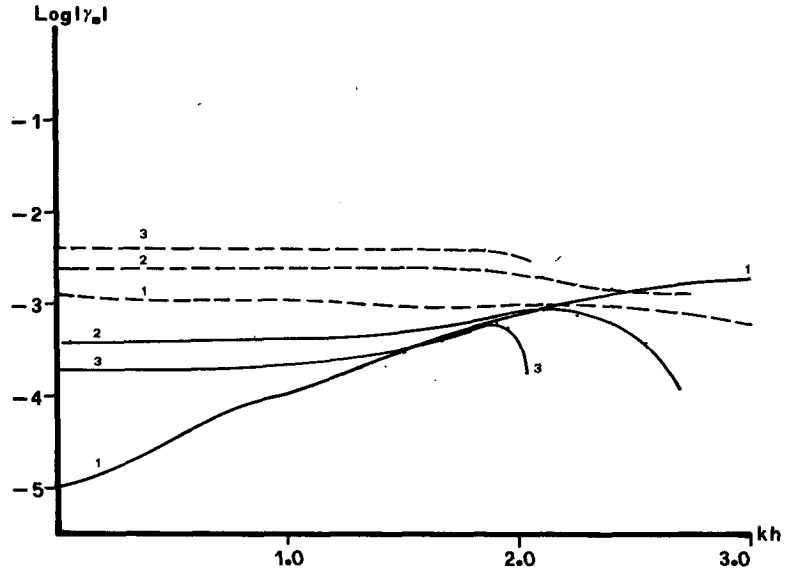

FIG. 10. Logarithm of the absolute values of the imaginary (solid lines) and real (dashed lines) parts of vertical wavenumbers as a function of the normalized horizontal wavenumber kh. The vertical wavenumbers are those corresponding to the modes of Fig. 2 in layer B.

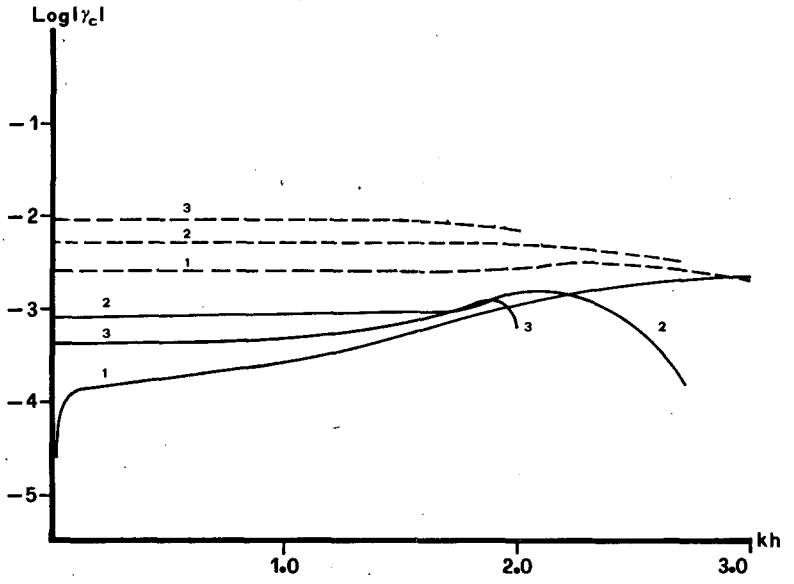

FIG. 11. As in Fig. 10 except in layer C.

case only those modes observed by Einaudi and Lalas (1974) when the jump in mean horizontal velocity and BV frequency are located at the same height are found by numerical analysis (see Fig. 8).

A possible role of the BV frequency jump is that of reflecting propagating neutral gravity waves; at the same time it is a well-known fact that when such internal waves meet a shear layer, overreflexion may take place if the horizontal phase speed of the disturbances satisfies the condition

$$-U<\frac{\omega}{k}<U. \tag{11}$$

This condition is always satisfied, for unstable disturbances described in the previous paragraph, at the velocity jump located at the interface between layers A and B. This is a consequence of the requirement that the semicircle theorem be satisfied.

If one then considers the system represented by the localized vortex sheet and the BV frequency jump represented in our model, it seems intuitively possible to imagine that waves, overreflected at the vortex sheet, can subsequently be returned to the overreflexion level because of the partial reflexion due to the presence of the BV frequency jump at $z=h$.

It is also rather obvious that such model, if associated with such a mechanism, would disappear if the BV

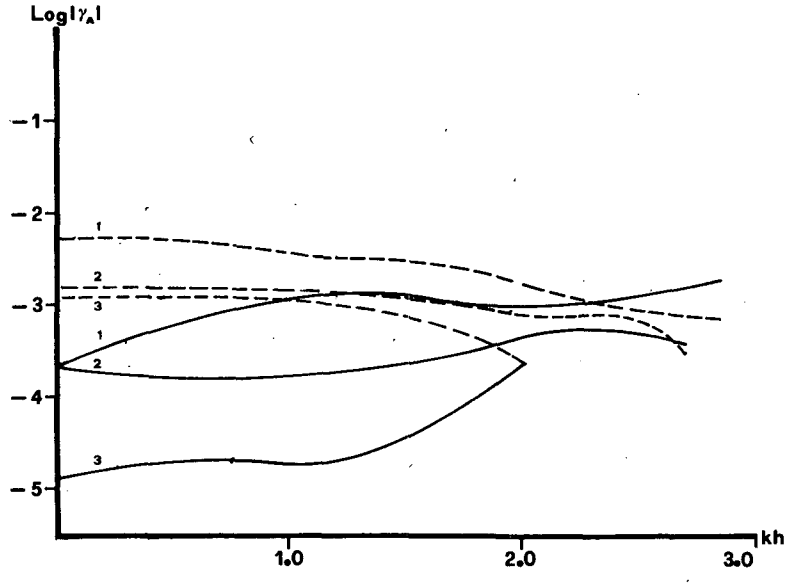

FIG. 12. As in Fig. 10 except in layer A.

frequency jump does not exist at $z=h$. In fact, in such a case, with over-reflexion at the shear layer, disturbances would not be returned to the overreflexion level (vortex sheet located at the interface between layers A and B) as no partial reflexion would take place at $z=h$. The reflexion coefficient at an interface where jumps in both mean horizontal velocity and BV frequency exist, can be written as

$$R=\left|\frac{A_r}{A_i}\right|=\left|\frac{1-\gamma_2(\omega/k-U_2)^2/\gamma_1(\omega/k-U_1)^2}{1+\gamma_2(\omega/k-U_2)^2/\gamma_1(\omega/k-U_1)^2}\right| \quad (12)$$

for neutrally propagating gravity waves. Here A_i and A_r are the amplitudes of the incident and reflected waves, respectively; γ_1 and γ_2 are the vertical wavenumbers of the solutions on the sides of the incident and transmitted waves, respectively; and U_1 and U_2 are the values of the horizontal velocity on the side of the incident and transmitted waves, respectively.

For a zero velocity jump, (12) reduces to

$$R=\left|\frac{\gamma_1-\gamma_2}{\gamma_1+\gamma_2}\right|\leqslant 1 \quad (13)$$

which, with the proper indexes, holds at the BV frequency jump of our model. If

$$(\omega/k-U_1)(\omega/k-U_2)<0, \quad (14)$$

then $R>1$ and overreflexion takes place. As stated previously, this condition is always satisfied for our unstable disturbances at the shear layer represented by the interface between layers A and B of our model.

We have further noticed that for unstable gravity modes and for the gravity-like extensions of the KH modes, the ratio

$$\frac{2\pi h}{\mathrm{Im}(\gamma_B)}$$

is always larger than unity (see the case of Fig. 10 when $N_1=10^{-2}$ s^{-1}, $U=5$ m s^{-1}, $h=1500$ m); this means that the oscillations along the vertical direction of the unstable disturbances are damped, in the layer B, on a length scale larger than h. One can interpret this fact as a further confirmation of the validity of our hypothesis because it suggests that unstable disturbances actually interact with the BV frequency jump located at $z=h$.

In a recent paper, Acheson (1976) has considered the problem of the stability of a two-vortex current sheet in a gently stratified fluid with constant BV frequency. In particular he analyzed unstable modes with associated small growth rates and showed that the growth rates of such disturbances can be approximately written as

$$\mathrm{Im}(\omega)=\frac{|w_g|}{2h}\ln(R_+R_-), \quad (15)$$

where $|w_g|$ is the magnitude of the vertical component of the group velocity in the intermediate layer, h the distance between the two jumps in mean horizontal velocity, R_- the reflexion coefficient for a downward neutral propagating gravity wave in the intermediate region incident on the lower velocity jump, and R_+ the reflexion coefficient for upward propagating waves in the intermediate region impinging the upper velocity jump.

As suggested by Acheson, Eq. (15) implies, in terms of normal mode theory, that such a disturbance will have been amplified by a factor $\exp[\mathrm{Im}(\omega)t]$ after a time t (see also Lindzen and Rosenthal, 1976). The application of this analysis to our model is straightforward and we refer to Appendix B of Acheson's paper. It should be noted that in our model the intermediate layer B is capped by the BV frequency jump (at the interface between layers B and C) and that, as a consequence, the reflexion coefficient for upward traveling gravity waves will be $\leqslant 1$ in such a layer.

A quantitative analysis of the estimate of the growth rates based on overreflexion coefficients is reported by Pellacani *et al.* (1977) in a more general case. It is shown that a good quantitative accord exists between numerical results and predictions obtained by (15).

An obvious consequence of (15) is that instabilities induced by such a mechanism of successive reflexions and overreflexions should have, for a fixed value of w_g, growth rates decreasing with increasing h. This result can be obtained directly by inspection of (15), and a physical explanation can be given if one takes into account the fact that two subsequent overreflexions will take place for a disturbance propagating upward and downward with a group velocity w_g, in a time interval given by $2h/w_g$. This consequence of (15) can hardly be simply verified for the disturbances considered here because of the quantization conditions in w_g; a more complete analysis is needed to explain the dependence of the growth rates on h for the different gravity modes. Some preliminary results have already been obtained and the problem will be considered in a future paper.

Two points are to be noticed: first, the maximum growth rate of the most unstable gravity mode is always located near $k=k_c$, where k_c is obtained introducing the values of N_1 and U into expression (1); and second, it has been shown by Lindzen and Rosenthal (1976) that in the case of a simple Helmholtz profile in an infinite Boussinesq fluid with constant BV frequency, neutral solutions exist for

$$\varphi_r=\mathrm{Re}(\varphi)=0, \quad (16a)$$

$$\varphi_r=\pm\left(\frac{N^2}{2k^2U^2}-1\right)^{\frac{1}{2}}. \quad (16b)$$

Careful inspection of Figs. 2–8 shows that φ_r and k corresponding to maximum φ_i of unstable gravity

modes, approximately satisfy the conditions (16a) and (16b) for $N=N_1$. There seems to be some connection then between unstable gravity modes and stable ones in the case when no BV frequency jump exists.

While the present work was in progress, Lindzen and Rosenthal (1976) and Lalas *et al.* (1976) published results on the instabilities induced by the presence of a rigid bottom on a Helmholtz velocity profile in a semi-infinite fluid with constant BV frequency. They showed that the presence of such a lower rigid boundary introduces new unstable modes in the range of long horizontal wavelengths. The modal structure of instabilities shown in Figs. 2 and 10–12 is particularly similar to that reported by Lindzen and Rosenthal. The BV frequency jump seems then to act analogously to a rigid lower bottom in creating a large number of unstable gravity modes. *A posteriori*, the analogy found between the effect of a rigid lower boundary and that of a BV frequency jump because of the capability of both elements in reflecting waves back to the overreflexion zone seems intuitively obvious. It is shown that, in particular conditions, growth rates associated with the most unstable gravity mode are greater than those associated with the KH gravity-like extensions in the range of low horizontal wavenumbers.

It should be noted that Figs. 2–8 and 10–12 show that the most unstable gravity modes have a growth rate smaller than those found by Lindzen and Rosenthal. This fact could be explained by the fact that the reflexion coefficient of a rigid boundary is always equal to unity while a BV frequency jump can give rise only to partial reflexion ($R<1$) in normal conditions.

Lalas and Einaudi (1976) considered a model in which an increase in the BV frequency above the velocity shear layer was considered together with a lower rigid bottom within the shear layer itself. They reported that the presence of the BV frequency jump did not affect substantially the growth rates of the unstable modes generated by the presence of the lower rigid boundary. Their results are easily understood by the comparison between our results on those reported by Lindzen and Rosenthal.

5. Applications to the atmosphere

As shown above, the net effect of the presence of a BV frequency jump far from the shear layer is the destabilization of disturbances with very long horizontal wavelengths. Such unstable disturbances can be associated with the most unstable gravity mode as well as with the gravity-like extensions of the KH mode depending on the particular situation (see Figs. 2 and 3). The ranges of the parameters considered in the previous sections have been chosen keeping in mind typical atmospheric situations. In this section, the discussion of the results is carried out in terms of the significant dimensional quantities h, N_1, N_2 and U rather than in terms of the nondimensional quantities α, β and r considered earlier.

Typical values of the BV frequency in the atmosphere range from zero to 4×10^{-2} s^{-1}, while localized vertical variations of the mean horizontal velocity range from a few meters per second to 10 m s^{-1}. Then, for reasonable values of h (from a few hundred meters to some kilometers), our values of the nondimensional parameters α and β corresponding to Figs. 2–8 turn out to be well representative of standard atmospheric configurations. On the other hand, our idealized model, when applied to the actual atmosphere, does not take into account any variation of the relevant physical quantities in the different layers and, in particular, in the intermediate one. Then, for too large values of h, the actual atmosphere is poorly suited to obtain significant results from our model. In this case, in fact, a variety of different possible phenomena such as wave absorption by turbulent layers, nonlinear effects, etc., can take place in the intermediate layer.

An interesting physical situation to which our analysis can be applied is the tropopause folding usually associated with cyclogenesis. In this case, in fact, since the stratosphere is characterized by much higher values of the BV frequency than in the atmosphere below, one could infer that the stability properties of preexisting tropospheric shear layers, now not too far from the BV frequency jump associated with the tropopause, would be affected in the sense considered above. Recent experimental results have shown that tropopause folding is actually associated with increase of instability phenomena in the atmosphere below. There seems to be, in particular, an effect of destabilization in the range of low horizontal wavenumbers (Klemp and Lilly, 1975). The effect we propose is a possible mechanism to explain the increasing of instability associated with tropopause folding. It is evident, however, that the lack of experimental data together with the coarseness of the model do not permit a definite confirmation of our hypothesis at this stage.

6. Conclusions

It has been shown that the presence of a BV frequency jump at a level different from that at which a localized shear zone exists can significantly affect the stability at the shear layer itself, particularly in the range of long horizontal wavelengths. The effect of the presence of such a BV frequency jump has been shown to be analogous to that of a lower rigid boundary. Particular agreement is found with the results given by Lindzen and Rosenthal (1976). The results obtained seem to confirm the importance of the overreflexion mechanism in the generation of such instabilities in the atmosphere. It is finally suggested that this effect can play a relevant role in the destabilization of preexisting tropospheric shear layers during tropopause folding events.

Acknowledgments. The authors would like to thank Dr. F. Einaudi for many fundamental discussions and Prof. A. Eliassen for his interesting suggestions.

APPENDIX

Numerical Method

To determine numerically the zeros of (8) for fixed values of k and h we made use of the two-dimensional false position method (Acton, 1970)

$$\varphi_{n+1}=\frac{\varphi_n y_{n-1}}{y_{n-1}-y_n}+\frac{\varphi_{n-1} y_n}{y_n-y_{n-1}}, \tag{A.1}$$

where φ_{n-1} and φ_n are trial complex values of the unknown φ in (8); y_{n-1} and y_n are the values on the left-hand side of (8) for $\varphi=\varphi_{n-1}$ and $\varphi=\varphi_n$, respectively; and φ_{n+1} represents the new estimate of the unknown φ. This method has been iterated until the convergence criterion

$$|\mathrm{Re}(y_n)|+|\mathrm{Im}(y_n)|<10^{-14} \tag{A.2}$$

was satisfied. In order to distinguish the zeros of (8) from minima of the order of 10^{-14}, we have considered only those numerical roots for which the real and the imaginary parts of the left-hand side of (8) changed their sign across the point taken as a root.

REFERENCES

Acheson, D. J., 1976: On over-reflexion. *J. Fluid Mech.*, **77**, 433–472.

Acton, F. S., 1970: *Numerical Methods that Work.* Harper and Row.

Bosart, L. F., and J. P. Cussen, 1973: Gravity wave phenomena accompanying East Coast cyclogenesis. *Mon. Wea. Rev.*, **101**, 446–454.

Chandrasekhar, S., 1961: *Hydrodynamic and Hydromagnetic Stability.* Clarendon Press (see pp. 482–483).

Davis, P. A., and W. R. Peltier, 1976: Resonant parallel shear instability in the stably stratified planetary boundary layer. *J. Atmos. Sci.*, **33**, 1267–1300.

Drazin, P. G., and L. N. Howard, 1966: Hydrodynamic stability of parallel flow of inviscid fluids. *Advances in Mechanics*, Vol. 9, Academic Press, 1–89.

Einaudi, F., and D. P. Lalas, 1974: Some new properties of Kelvin-Helmholtz waves in the atmosphere with and without condensation effects. *J. Atmos. Sci.*, **31**, 1995–2007.

Helmholtz, H., 1868: Ueber Discontinuirliche Flüssigkeits-bewegungen. *Monats. Königl. Preuss. Acad. Wiss. Berlin*, 215–228 [Translation by F. Gutrie, 1868: On discontinuous movements of fluids. *Phil. Mag.*, **36**, 337–346.]

Howard, L. N., 1961: Note on a Paper of John W. Miles. *J. Fluid Mech.*, **10**, 509–512.

Keliher, T. E., 1975: The occurrence of microbarograph-detected gravity waves compared with the existence of dynamically unstable wind shear layers. *J. Geophys. Res.*, **80**, 2967–2976.

Klemp, J., and D. K. Lilly, 1975: The dynamics of wave-induced downslope winds. *J. Atmos. Sci.*, **32**, 320–329.

Lalas, D. P., and F. Einaudi, 1976: On the characteristics of gravity waves generated by atmospheric shear layers. *J. Atmos. Sci.*, **33**, 1248–1259.

——, ——, and D. Fua, 1976: The destabilizing effect of the ground on Kelvin-Helmholtz waves in the atmosphere. *J. Atmos. Sci.*, **33**, 59–69.

Lindzen, R. S., 1974: Stability of a Helmholtz velocity profile in a continuously stratified, infinite, Boussinesq fluid-applications to clear-air turbulence. *J. Atmos. Sci.*, **31**, 1507–1514.

——, and A. J. Rosenthal, 1976: On the instability of Helmholtz velocity profiles in stably stratified fluid when a lower boundary is present. *J. Geophys. Res.*, **81**, 1561–1571.

Ludlam, F. H., 1967: Characteristics of billow clouds and their relation to clear-air turbulence. *Quart. J. Roy. Meteor. Soc.*, **93**, 419–435.

Pellacani, C., C. Tebaldi and E. Tosi, 1977: On the instabilities induced by over-reflexion in stratified fluids in horizontal sheared motion. Submitted to *Phys. Fluids.*

Sekioka, M., 1970: Application of Kelvin-Helmholtz instability to clear-air turbulence. *J. Appl. Meteor.*, **9**, 896–899.

Uccellini, L. W., 1973: A case study of apparent gravity wave initiation of severe convective storms. Rep. N. 73-2, NSF Grant GI-31278X, University of Wisconsin.